PHOTONIC SENSORS / Vol. 4, No. 3, 2014: 281–288

Response Analysis of Ultrasonic Sensing System Based on Fiber Bragg Gratings of Different Lengths

Dandan PANG and Qingmei SUI*

School of Control Science and Engineering, Shandong University, Jinan, 250061, China

*Corresponding author: Qingmei SUI E-mail: pangdan58@163.com

Abstract: In recent years, fiber Bragg gratings (FBGs) have been widely used in ultrasonic detection for practical structural health monitoring in light of its unique advantages over the conventional sensors. Although FBGs have been successfully tested in ultrasonic inspection, the effect of the grating length on the sensitivity of the FBG ultrasonic sensing system is yet to be analyzed. Hence, using the simulation model, the main influencing factor on the sensitivity of the ultrasonic sensing system with different lengths gratings was first investigated. In the following experiment, the ultrasonic responses of the sensing system with six different lengths FBGs were obtained, respectively. The theoretical analysis and the experimental results would be useful for sensitivity improvement of the FBG-based ultrasonic and acoustic emission sensing system.

Keywords: Fiber Bragg gratings, Bragg reflectors, optical sensing and sensors

Citation: Dandan PANG and Qingmei SUI, "Response Analysis of Ultrasonic Sensing System Based on Fiber Bragg Gratings of Different Lengths," *Photonic Sensors*, 2014, 4(3): 281–288.

1. Introduction

Ultrasonic inspection plays an important role in structure health monitoring (SHM), industrial safety monitoring, automotive, aerospace, and therapeutic applications due to its high sensitivity to both surface and subsurface discontinuities as well as its highly accuracy in determining the position, shape, and size of the reflector [1, 2]. Ultrasonic sensors based on fiber Bragg gratings (FBGs) have many advantages over classical piezoelectric sensors, including the immunity to electromagnetic interference, small size, lightweight, multiplexity, and capability to be embedded in the monitoring structure [3–5].

FBGs-based ultrasonic sensors are good candidates for detecting ultrasonic waves due to the aforementioned advantages. The FBG ultrasonic sensing system typically relies on detecting an intensity shift of light reflected from the FBG caused by ultrasonic waves using a narrow line-width laser locked to the wavelength at the full width at half maximum (FWHM) [6]. The sensitivity of this sensing system is limited by the wavelength shifting amplitude and the spectral slope of the linear range [7]. The influencing factors on the sensitivity of FBG ultrasonic sensors and the methods of sensitivity enhancement in intensity-modulated FBG ultrasonic or vibration sensors have been extensively studied in recent years [7–11]. Minardo *et al.* [8] modeled the ultrasonic waves and FBG interaction taking both geometric and elasto-optic effects into account for uniform and apodized FBGs, and numerically analyzed the key parameter of the ratio between the ultrasonic

Received: 9 December 2013 / Revised version: 15 January 2014

DOI: 10.1007/s13320-014-0157-4
Article type: Regular

wavelength and the grating length affecting the FBG response to an ultrasonic wave. Betz *et al*. [9] studied the influence of the acoustic wavelength and amplitude on the grating spectrum, and experiments were carried out to validate the responses of FBGs of different lengths to the incident acoustic waves. However, in those studies, the effect of the spectral slopes of FBGs with different lengths on the sensitivity of the overall system has been neglected.

To address the problem mentioned above, in this work, the slopes of the linear range in the FBGs reflection spectra have been taken into account to investigate the response of gratings with different lengths to ultrasonic waves. Using the traditional transfer matrix method, the output of the ultrasonic detecting system with the narrowband interrogation method has been modeled. Response analysis has been performed for systems with different lengths gratings. Experiments were carried out to demonstrate the optimum grating length for ultrasonic inspection on an aluminum plate. The obtained results are believed to be of great value for the optimization design of the FBGs-based ultrasonic sensing system.

2. Ultrasonic sensing principle of FBG and sensitivity response of ultrasonic sensing system with FBGs of different lengths

2.1 Ultrasonic sensing principle of FBG

To study the interaction between an FBG and an ultrasonic wave, the time-dependent ultrasonic strain is modeled according to

$$\varepsilon(t) = A_{\mathrm{US}} \cos(\frac{2\pi}{\lambda_{\mathrm{US}}} z - \omega_{\mathrm{US}} t) \tag{1}$$

where A_{US} denotes the ultrasonic wave amplitude normalized to the ultrasonic wavenumber $2\pi/\lambda_{\mathrm{US}}$, λ_{US} is the wavelength, and ω_{US} is the angular frequency of the ultrasonic wave, respectively. Here, z is the point along the fiber axis, and the limit of the grating length is defined as $0 \le z \le L$.

An ultrasonic wave causes a refractive index change via the strain-optic effect and induces geometrical deformation along the FBG [12, 13]. Taking the two effects mentioned into account, the Bragg effective refractive index modulation under the ultrasonic wave can be expressed as [14]

$$n'_{\mathrm{eff}}(z',t) = n_{\mathrm{eff0}} - \Delta n \sin^2(\frac{\pi}{\Lambda_0} z) - \frac{n_{\mathrm{eff0}}^3}{2} \cdot [P_{12} - \nu(P_{11} + P_{12})] \cdot A_{\mathrm{US}} \cos(\frac{2\pi}{\lambda_{\mathrm{US}}} z' - \omega_{\mathrm{US}} t) \tag{2}$$

where n_{eff0} is the original effective refractive index, Δn is the maximum index change, Λ_0 is the grating period, P_{ij} are the stress-optic coefficients, ν is the Poisson's ratio, and z' is the new point along the fiber axis due to the geometrical deformation, which can be obtained as

$$z' = z + \int_0^z \varepsilon(\xi) d\xi = z + A_{\mathrm{US}} \frac{\lambda_{\mathrm{US}}}{2\pi} \sin(\frac{2\pi}{\lambda_{\mathrm{US}}} z - \omega_{\mathrm{US}} t) + A_{\mathrm{US}} \frac{\lambda_{\mathrm{US}}}{2\pi} \sin(\omega_{\mathrm{US}} t). \tag{3}$$

2.2 Simulation of the sensitivity response of ultrasonic sensing system with FBGs of different lengths

A. Simulation principle

Figure 1 shows the simulated reflection spectra of gratings with different lengths. The parameters of the gratings used in the simulation were obtained from the spectral responses of realistic gratings of different lengths. The grating lengths were 1 mm, 2 mm,

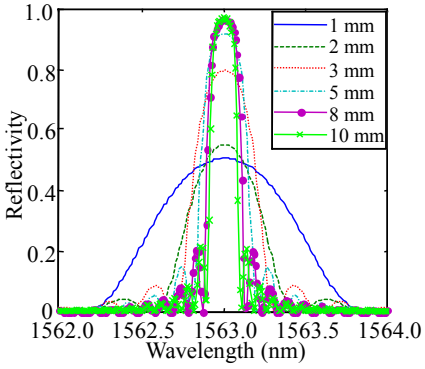

Fig. 1 Simulated reflected spectra of gratings with different lengths.

3 mm, 5 mm, 8 mm, and 10 mm, and the corresponding FWHM bandwidths were 1.13 nm, 0.61 nm, 0.59 nm, 0.55 nm, 0.40 nm, and 0.26 nm. As shown in Fig. 1 clearly, a longer grating length was always accompanied with a higher reflectivity and a steeper slope.

With the narrowband laser interrogation method, the laser was set to the wavelength at the FWHM of the grating, and the grating subjected to ultrasonic waves was demodulated by the reflected intensity variations. The interrogation principle of gratings with different lengths under ultrasonic waves is shown in Fig. 2(a), taking a 1-mm-length grating and a 5-mm-length grating for examples. However, it is worthy of note that this interrogation method is only applicable when part of the grating spectrum can be assumed to be linear. The required linearity occurs in reflectivity between 20% and 80% of an FBG reflection spectrum. When the ultrasonic wave amplitude exceeds 15 με (Fig. 3), the wavelength of the laser will extend out the linear region of the grating spectrum. Therefore, it should be noted that the applied ultrasonic wave amplitude cannot exceed 15 με.

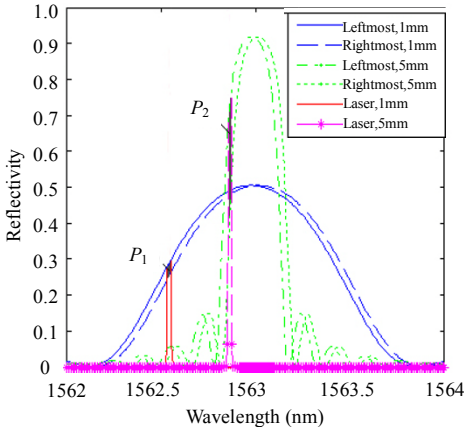

(a)

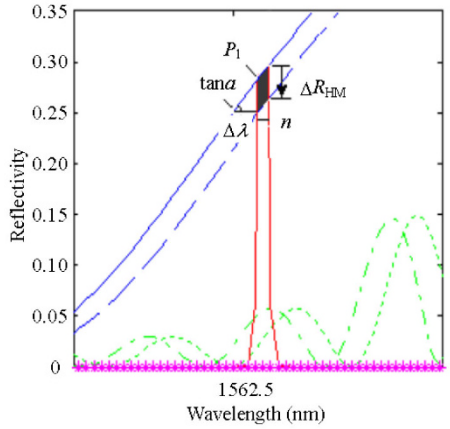

(b)

Fig. 2 Interrogation principle of the grating under ultrasonic wave with the amplitude of 15 με and frequency of 150 kHz: (a) simulated leftmost spectrum with the minimum wavelength and rightmost spectrum with the maximum wavelength in an ultrasonic period of a 1-mm-length grating and a 5-mm-length grating and (b) enlarged spectrum.

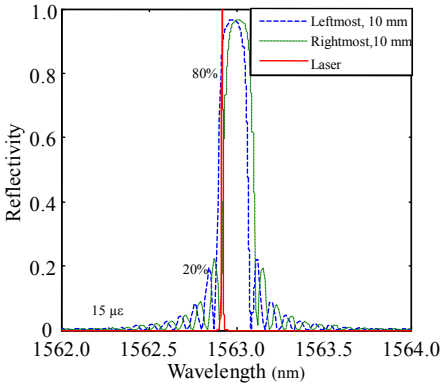

Fig. 3 Simulated leftmost and rightmost spectra of a 10-mm-length grating subjected to an ultrasonic wave with amplitude of 15 με.

Figure 2(a) clearly shows the simulated leftmost spectrum with the minimum wavelength and rightmost spectrum with the maximum wavelength in one ultrasonic period of a 1-mm-length grating and a 5-mm-length grating subjected to an applied ultrasonic wave with an amplitude of 15 με and a frequency of 150 kHz, respectively. Here, in Fig. 2(a, the gray areas represent the peak-to-peak amplitudes of the reflected intensity variations induced by the grating spectra shifts. Each gray area can be assumed as a parallelogram due to the ultra-narrow bandwidth of the laser, as shown in Fig. 2(b). Therefore, the gray areas P_1 and P_2 can be approximately represented by (4)

$$\begin{aligned} P_i &= P_{\text{left}i} - P_{\text{right}i} \\ &= \Delta R_{\text{HM}i} \cdot n = \Delta\lambda_i \cdot \tan\alpha_i \cdot n \qquad i = 1,2 \end{aligned} \tag{4}$$

where $P_{\text{left}i}$ is the reflected intensity of the leftmost spectrum in an ultrasonic period; $P_{\text{right}i}$ is the reflected intensity of the rightmost spectrum in an ultrasonic period; n= 4×10^{-4}pm is the bandwidth of

the laser; $\Delta R_{\mathrm{HM}i}$ is the maximal amplitude change in the reflectivity of the FBG at the set laser wavelength in one ultrasonic period; $\Delta\lambda_i$ is approximately equal to the wavelength shift of the FBG; and $\tan\alpha_i$ is the spectrum slope of the FBG.

Here, we assume $P_{0i}=(P_{\mathrm{left}i}+P_{\mathrm{right}i})/2$ as the initial light intensity in the ultrasonic period. From (4), the intensity sensitivity S_{Pi} can be obtained as follows:

$$S_{Pi}=\frac{P_i}{P_{0i}}=\frac{2\cdot\Delta R_{\mathrm{HM}i}}{(R_{\mathrm{left}i}+R_{\mathrm{right}i})}=\frac{\Delta\lambda_i\cdot\tan\alpha_i}{R_{0i}} \qquad i=1,2. \tag{5}$$

Equation (5) describes the calculation method of the intensity sensitivity of the entire system. According to (5), the intensity sensitivity depends on the wavelength shift $\Delta\lambda_i$, the slope of the FBG $\tan\alpha_i$, and the initial reflectivity of the FBG at the set laser wavelength R_{0i}.

B. Simulation results

In order to find out the main influencing factor on the sensitivity of the tunable laser-based interrogation system, the relationship among the sensitivity S_p, the wavelength shift $\Delta\lambda$, the slope of FBG $\tan\alpha$, and the initial reflectivity of the grating spectrum at the set laser wavelength R_0 was studied by numerical simulations. Figure 4(a) shows the maximal reflectivity change in the grating spectrum at the set laser wavelength in one ultrasonic period ΔR_{HM}, as a function of the FBG length. Evidently, ΔR_{HM} increases almost linearly with an increase in the FBG length. Figure 4(b) displays the shift of the grating wavelength $\Delta\lambda$ in one ultrasonic period for the grating length ranging from 1 mm to 10 mm. In agreement with the results observed by Minardo *et al*. [6], the maximal wavelength shift $\Delta\lambda$ decreases with an increase in the FBG length, except for one abnormal point at the FBG length 3 mm. This can be attributed to the sudden rise of the spectrum slope of the 3-mm-length FBG. From Figs. 4(a) and 4(b), one can see the changing trends of ΔR_{HM} and $\Delta\lambda$ are in opposite directions, and according to (4), the conclusion that the dominant influencing factor of ΔR_{HM} is the spectrum slope of the FBG $\tan\alpha$ can be obtained.

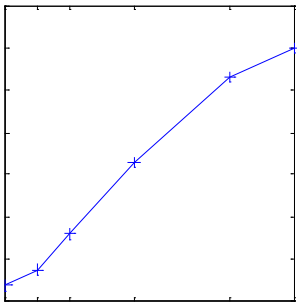

(a)

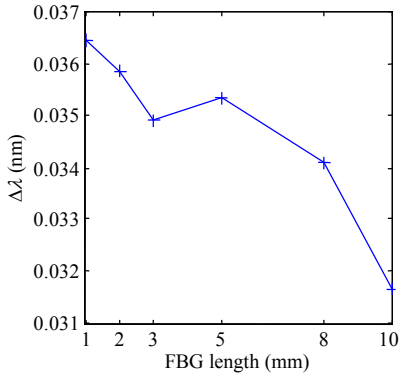

(b)

Fig. 4 Relationship between the maximal reflectivity change ΔR_{HM} and the shift of the grating wavelength $\Delta\lambda$: (a) variation of the maximal reflectivity change ΔR_{HM} with the FBG length and (b) simulation results for the shift of the grating wavelength $\Delta\lambda$ versus the FBG length.

The relationship between the initial reflectivity of the grating spectrum at the set laser wavelength R_0 and FBG length is shown in Fig. 5. R_0 is calculated by averaging the reflectivity of the leftmost grating spectrum at the set laser wavelength (the maximum reflectivity in one ultrasonic period) R_{left} and the reflectivity of the rightmost grating spectrum at the set laser wavelength (the minimum reflectivity in one ultrasonic period) R_{right}. According to Fig. 5, R_0 increases with an increase in the FBG length.

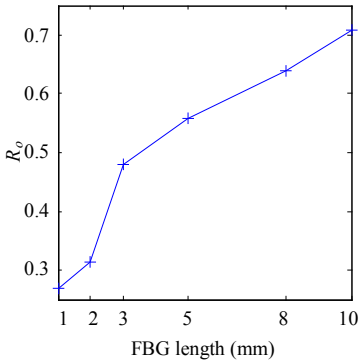

Fig. 5 Relationship between the initial reflectivity of the grating spectrum at the set laser wavelength R_0 and FBG length.

Figure 6 shows the intensity sensitivity of the entire sensing system S_p as a function of the FBG length for an ultrasonic wave amplitude of 15 με. S_p is calculated from dividing the peak-to-peak amplitude of the reflected intensity variation P by the initial light intensity in the ultrasonic period P_o, according to (5). The simulation results show that the intensity sensitivity increases significantly with an increase in the FBG length at low values of the FBG length. The intensity sensitivity at the 8-mm FBG length is close to that at the 10-mm FBG length. For the system with a 10-mm-length FBG, the sensitivity reaches a peak of 0.85. These results reveal that the intensity sensitivity of the system is significantly affected by the spectrum slope of the FBG $\tan\alpha$.

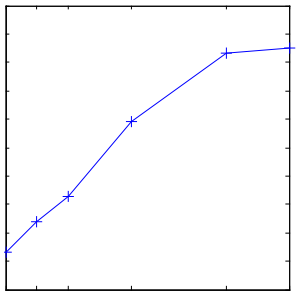

Fig. 6 Intensity sensitivity of the system S_p versus the FBG length.

3. Experiments and results

The experimental setup of the FBG-based ultrasonic sensing system is demonstrated in Fig. 7. A narrowband piezoelectric transducer (PZT) with a resonance frequency of 150 kHz was connected to a waveform generator. The waveform generator produced modulated sinusoidal pulses with the amplitude of 1 V – 5 V, propagating through a 3-mm-thickness aluminum alloy plate. A narrowband tunable semiconductor laser (TSL) with the line-width of 100 kHz and the wavelength resolution of 1 pm was tuned to the FWHM point of the sensing FBG to obtain the optimum sensitivity, and its output power was set to 5 mW. The FBGs were fabricated with parameters representing the

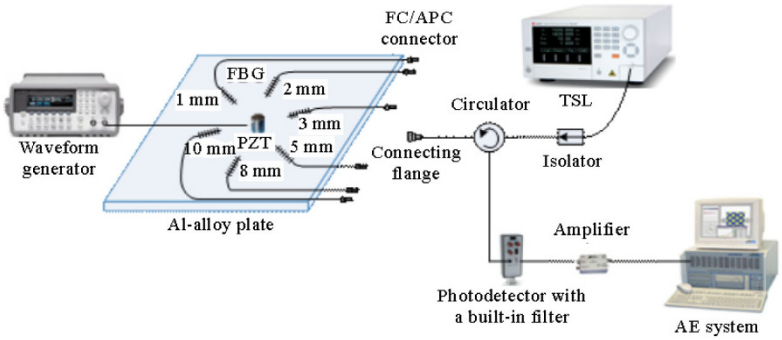

Fig. 7 Experimental setup of the FBG-based ultrasonic sensing system.

numerical simulation. A circulator guided the reflected light from the FBG to a photodetector with a built-in band-pass filter. The converted electrical voltages were filtered by the band-pass filter (100 kHz – 300 kHz) and then entered an acoustic emission (AE) preamplifier. The AE system monitored the response of the FBG by recording the intensity of the acoustic signal. As shown in Fig. 8, the FBGs and the PZT were all surface-attached to the aluminum alloy plate. All gratings were placed at

an equal distance (200 mm) from the PZT in order to ensure the same acoustic amplitude. Figure 9 shows the reflected spectrum of the 10-mm-length FBG free of the acoustic wave.

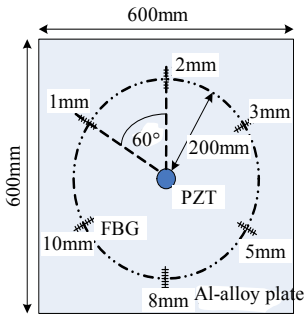

Fig. 8 Layout of different lengths FBGs on the aluminum alloy plate.

In this experiment, gratings of different lengths were attached to the sensing system by jointing the angled physical contact connector (FC/APC) in each channel with the flange. In order to characterize the responses of gratings with different lengths, the amplitude of the ultrasonic wave generated by the PZT was fixed at 3 V, and the amplitude of the ultrasonic signal applied to gratings was about 15 με.

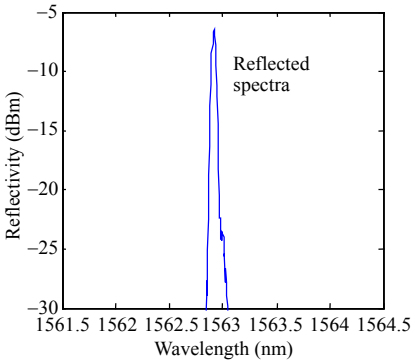

Fig. 9 Reflected spectrum of the 10-mm-length FBG used in the experiment.

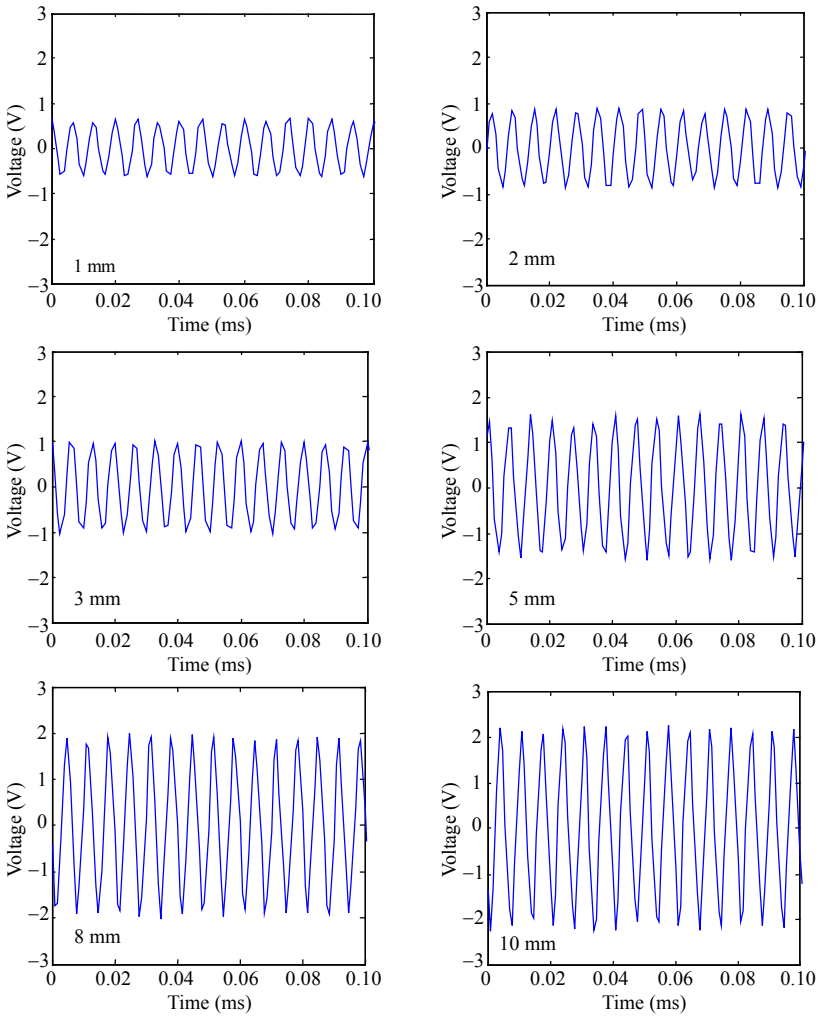

Fig. 10 Comparison of time responses of gratings of different lengths under the same excitation signal.

If the FBGs suffered from surrounding temperature changes, the wavelength of the laser would not set at the preset operating point, even worse might extend out the operating linear region of the grating spectrum (especially the 10-mm-length FBG). In order to make sure the experiment goes well, we should eliminate the effects of temperature changes. During the experiment, the room temperature was monitored and held constantly at 18 ℃. The reflected optical power before entering the photodetector was detected at a ten-minute interval to ensure the preset operating point remained unchanged. Therefore, the optimum sensitivity could be obtained throughout the experiment.

The time-varying acoustic signals recorded by the AE system were used to compare the response sensitivity of the system with gratings of different lengths. As shown in Fig. 10, the amplitudes of detected acoustic signals increase gradually with an increase in the grating lengths. There is an abrupt increase in the amplitude of the response waveform of the 5-mm-length FBG. The response amplitudes of the 8-mm and 10-mm gratings are almost the same. The relationship between the normalized FBG response and the grating length is shown in Fig.11. The result in Fig. 11 is consistent with the numerical result in Fig. 6. Obviously, the maximum amplitude of the FBG response can be achieved at the grating length of 10 mm.

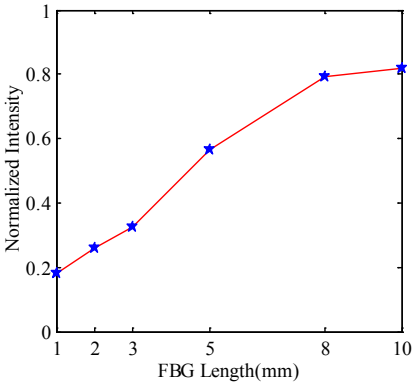

Fig. 11 Normalized optical signal strength plotted with respect to the FBG length.

4. Conclusions

In this paper, the grating length dependence of the fiber Bragg grating based ultrasonic sensing system was investigated theoretically and experimentally. Firstly, an efficient sensitivity equation of the ultrasonic detecting system was established. Then, in the numerical simulation part, the slope of the FBG spectrum as a key parameter affecting the sensitivity was highlighted. Simulations show that, for a given ultrasonic wave with a less-than-15-με amplitude acting on the grating, the intensity sensitivity of the system can be enhanced by increasing the FBG length as the increased slope of the FBG spectral linear range overcomes the reduced wavelength sensitivity from a longer grating length. Finally, an ultrasonic detecting system with gratings of different lengths was built to experimentally demonstrate the theoretical finding. The time responses of the gratings with lengths ranging from 1 mm to 10 mm were obtained, and the measurement results agreed well with the theoretical analysis. This concluded that the sensitivity of the system was primarily determined by the slope of the FBG spectral linear range. The theoretical and experimental results provided an optimal system design for ultrasonic detecting.

Acknowledgment

The authors gratefully acknowledge the financial support for this work from the Natural Science Foundation of China (Grant No. 61074163) and the Natural Science Foundation of Shandong Province, China (Grant No. ZR2011FQ025).

References

[1] D. Clorennec, C. Prada, and D. Royer, “Laser

ultrasonic inspection of plates using zero-group velocity lamb modes," *IEEE Transactions on Ultrasonics, Ferroelectrics and Frequency Control*, 2010, 57(5): 1125–1132.

[2] C. J. Lane, A. K. Dunhill, B. W. Drinkwater, and P. D. Wilcox, "The inspection of anisotropic single-crystal components using a 2-D ultrasonic array," *IEEE Transactions on Ultrasonics, Ferroelectrics and Frequency Control*, 2010, 57(12): 2742–2752.

[3] Y. J. Rao, "In-fiber Bragg grating sensors," *Measurement Science & Technology*, 1997, 8(4): 355–375.

[4] J. R. Lee and C. Y. Yoon, "Development of an optical system for simultaneous ultrasonic wave propagation imaging at multi-points," *Experimental Mechanics*, 2010, 50(7): 1041–1049.

[5] A. Rosenthal, D. Razansky, and V. Ntziachristos, "High-sensitivity compact ultrasonic detector based on a pi-phase-shifted fiber Bragg grating," *Optics Letters*, 2011, 36(10): 1833–1835.

[6] B. Lissak, A. Arie, and M. Tur, "Highly sensitive dynamic strain measurements by locking lasers to fiber Bragg gratings," *Optics Letters*, 1998, 23(24): 1930–1932.

[7] A. I. Azmi, D. Sen, W. Sheng, J. Canning, and G. D. Peng, "Performance enhancement of vibration sensing employing multiple phase-shifted fiber Bragg grating," *Journal of Lightwave Technology*, 2011, 29(22): 3453–3460.

[8] A. Minardo, A. Cusano, R. Bernini, L. Zeni, and M. Giordano, "Response of fiber Bragg gratings to longitudinal ultrasonic waves," *IEEE Transactions on Ultrasonics, Ferroelectrics and Frequency Control*, 2005, 52(2): 304–312.

[9] D. C. Betz, G. Thursby, B. Culshaw, and W. J. Staszewski, "Identification of structural damage using multifunctional Bragg grating sensors: I. theory and implementation," *Smart Materials and Structures*, 2006, 15(5): 1305–1312.

[10] Z. Li, L. Pei, B. Dong, C. Ma, and A. Wang, "Analysis of ultrasonic frequency response of surface attached fiber Bragg grating," *Applied Optics*, 2012, 51(20): 4709–4714.

[11] T. Liu and M. Han, "Analysis of π-phase-shifted fiber Bragg gratings for ultrasonic detection," *IEEE Sensors Journal*, 2012, 12(7): 2368–2373.

[12] A. D. Kersey, M. A. Davids, H. J. Patrick, M. Leblanc, K. P. Koo, C. G. Askins, *et al.*, "Fiber grating sensors," *Journal of Lightwave Technology*, 1997, 15(8): 1442–1463.

[13] G. Wild and S. Hinckley, "Acousto-ultrasonic optical fiber sensors: overview and state-of-the-art," *IEEE Sensors Journal*, 2008, 8(7): 1184–1193.

[14] V. Italia, A. Cusano, S. Campopiano, A. Cutolo, and M. Giordano, "Analysis of the phase response of fiber Bragg gratings to longitudinal ultrasonic fields in the high frequency regime: towards new interrogation strategies," *Proceedings of 2005 IEEE/LEOS Workshop on Fibers and Optical Passive Components*, Italy, June 22–24, pp. 389–392, 2005.